

1 Disclaimer: This preprint has been submitted for publication to a peer-reviewed journal. All  
2 original descriptions in this bioRxiv document are not issued for public and permanent  
3 scientific record, or for purposes of zoological nomenclature. The new species name  
4 mentioned in this document will only become available with the proper publication of the  
5 article.

6  
7  
8 **New fossil wasp species from the earliest Eocene Fur Formation has its closest relatives in**  
9 **late Eocene ambers (Hymenoptera, Ichneumonidae, Pherhombinae)**

10  
11 Noah Meier<sup>\*1,2</sup>, Anina Wacker<sup>\*3</sup>, Seraina Klopfstein<sup>1,4</sup>

12 \*these two authors contributed equally

13 <sup>1</sup>Naturhistorisches Museum Basel, Augustinergasse 2, CH-4001 Basel, Switzerland

14 <sup>2</sup>University of Basel, Department of Environmental Sciences – Section of Conservation  
15 Biology, St. Johanns-Vorstadt 10, 4056 Basel

16 <sup>3</sup>University of Basel, Department of Environmental Sciences – Plants, Schönbeinstrasse 6,  
17 CH-4056 Basel

18 <sup>4</sup>Institute of Ecology and Evolution, University of Bern, Baltzerstrasse 6, CH-3012 Bern,  
19 Switzerland

20  
21 Correspondence: [seraina.klopfstein@bs.ch](mailto:seraina.klopfstein@bs.ch)

22  
23  
24  
25  
26  
27  
28  
29 **Abstract**

30 Darwin wasps (Ichneumonidae) are one of the most species-rich insect families, but also one  
31 of the most understudied ones, both in terms of their extant and extinct diversity. We here  
32 use morphometrics of wing veins and an integrative Bayesian analysis to place a new rock  
33 fossil species from the Danish Fur Formation (~54 Ma) in the tree of Darwin wasps. The new  
34 species, *Pherhombus parvulus* n. sp., is placed firmly in Pherhombinae, an extinct subfamily  
35 so far only known from Baltic and Rovno-Ukrainian ambers, which are estimated to be 34–48  
36 Ma and 34–38 Ma, respectively. Our phylogenetic analysis recovers a subfamily clade within  
37 the higher Ophioniformes formed by Pherhombinae, Townesitinae and Hybrizontinae, in  
38 accordance with previous suggestions. Due to the placement of the new species as sister to  
39 the remaining members of Pherhombinae, we argue that our finding is not at odds with a  
40 much younger, late Eocene age (~34–41 Ma) of Baltic amber and instead demonstrates that  
41 *Pherhombus* existed over a much longer period than previously thought. Our results also  
42 exemplify the power of wing vein morphometrics and integrative phylogenetic analyses in  
43 resolving the placement even of poorly preserved fossil specimens.

44  
45 **Keywords:** Bayesian phylogenetic inference, compression fossil, morphometrics, parasitoid  
46 wasps, phylogeny

47  
48

49

50 Insect taxonomy in the past centuries was strongly biased towards large and colourful  
51 species and thus overrepresented Lepidoptera and Coleoptera. More recently, other orders  
52 came into focus, especially Diptera and Hymenoptera, due to their extraordinary diversity  
53 and ecological and economic importance (Forbes et al. 2018, Ronquist et al. 2020). Among  
54 them, Darwin wasps (Ichneumonidae) are assumed to have one of the largest gaps between  
55 the number of described species and the actual species diversity (Klopfstein et al. 2019b).  
56 The fossil record of ichneumonids goes back to the Lower Cretaceous, about 120-130 Ma,  
57 while a recent dating study placed the origin of the family and most of its subfamilies in the  
58 Jurassic (about 181 Ma; Spasojevic et al. 2021). However, the fossil record of Darwin wasps is  
59 even more under-researched than their extant diversity, which impedes inferences about  
60 their past diversity and evolutionary history. In this study, we describe an approximately 54  
61 Ma old ichneumonid rock fossil species from the Danish Fur Formation (Rust 1998). Its  
62 forewing venation with a large, rhombic areolet is rather rare among members of the family,  
63 both extant and extinct, and makes it unique among the known Fur Formation  
64 ichneumonids.

65

#### 66 *Darwin Wasp Fossils from the Early Eocene Fur Formation*

67 The Fur Formation is located in northwestern Jutland in Denmark, with its center on  
68 the islands of Fur and Mors. The 60 m thick sediments consists of porous diatoms and  
69 contains approximately 200 volcanic ash layers that were deposited right after the  
70 Paleocene-Eocene Thermal Maximum, about 54 Ma (Chambers et al. 2003, Westerhold et al.  
71 2009). It is one of the oldest Cenozoic deposits of fossil insects in Europe (Larsson 1975) and  
72 interestingly, only winged insect forms have been found so far (Rust 1998). This is probably  
73 due to the distance of 100 km from the Scandinavian coastal line at the time of deposition.  
74 The recovered insects were either blown onto the open sea by storms (Larsson 1975) or  
75 showed long-distance migratory behavior (Ansorge 1993, Rust 2000). Rust (1998) mentioned  
76 two forms of Darwin wasps that were common among Fur insects: one dark, strongly  
77 sclerotized and one light, less sclerotized form. However, more recent work showed that  
78 these forms each included multiple species (Klopfstein in press). Currently, there are ten  
79 Darwin wasp species known from Fur, all of which are classified in the extant subfamily  
80 Pimplinae (Henriksen 1922, Klopfstein in press). So far, no species from any of the other 41  
81 extant and five extinct subfamilies have been recorded from Fur, even though preliminary  
82 analyses indicate a much higher diversity (own observations). Given that Darwin wasps have  
83 recently been estimated to date back to the Jurassic (~181 Ma) and most extant subfamilies  
84 have probably started diversifying by the Early Cretaceous (>100.5 Ma; Spasojevic et al.  
85 2021), a much higher diversity would also be expected for the early Cenozoic.

86

#### 87 *Candidate subfamilies: Mesochorinae and Pherhombinae*

88 The forewing venation of the fossil in question, especially the rhombic areolet,  
89 suggests that the new fossil species belongs to either the extant Mesochorinae or the extinct  
90 Pherhombinae (Broad et al. 2018). With 863 extant and 8 fossil species (Yu et al. 2016),  
91 Mesochorinae are quite a large subfamily. Typical features include a straight, needle-like  
92 ovipositor, in most cases a large rhombic areolet, a deep glymma in the first metasomal  
93 segment, and extended, rod-like parameres in the male. As far as we know, Mesochorinae  
94 are obligate hyperparasitoids, using mostly Ichneumonidae and Braconidae larvae as primary  
95 hosts (Broad et al. 2018). Brues (1910) described eight fossil Mesochorinae species from the  
96 Florissant Formation, approximately 34 Ma (McIntosh et al. 1992) and one species from

97 Baltic amber (Brues 1923). This latter species was later transferred to Pherhombinae, an  
98 extinct subfamily described more recently (Kasparyan 1988).

99 The monotypic Pherhombinae was established based on two species from Baltic  
100 amber, *Pherhombus antennalis* Kasparyan, 1988 and *P. brischkei* (Brues, 1923). In 2005,  
101 Tolkanitz et al. described *P. dolini*, the first Pherhombinae found in Ukrainian Rovno amber  
102 (Tolkanitz et al. 2005). And recently, Manukyan (2019) described three further *Pherhombus*  
103 species from Baltic amber, increasing the number of species in the subfamily to six.  
104 Kasparyan (1988, 1994) proposed a close relationship of Pherhombinae with the extinct  
105 Townesitinae and the extant Hybrizontinae and cited several character states as potential  
106 synapomorphies for this clade. In a recent phylogenetic analysis that included one species of  
107 Pherhombinae (*P. antennalis*), this grouping was indeed recovered among other subfamilies  
108 of the Ophioniformes group, although with a very sparse taxon sampling (Spasojevic et al.  
109 2021). Interestingly, Manukyan (2019) suggested a crepuscular or nocturnal activity for the  
110 subfamily based on the somewhat enlarged, raised ocelli. As all extant subfamilies that  
111 include nocturnal species (Ophioninae, Mesochorinae, Tryphoninae and Ctenopelmatinae)  
112 belong to Ophioniformes, the placement of Pherhombinae in this group appears plausible.  
113 Regarding the biology of Pherhombinae, only little is known otherwise, although their short  
114 ovipositor might indicate that they attack exposed hosts, for instance larvae of Lepidoptera  
115 or Symphyta (Belshaw et al. 2003).

116  
117 *Amber fossils and their controversial age*

118 All Pherhombinae described so far were found as inclusions in Baltic and Rovno  
119 amber (Manukyan 2019). Age estimates of Baltic amber vary considerably (about 56.0 to  
120 33.9 Ma: Ritzkowski 1997, Perkovsky et al. 2007, Bukejs et al. 2019); they are based on  
121 biostratigraphic analyses (pollen, spores, phytoplankton), lithographic analyses of  
122 surrounding sediment, and K-Ar age estimation of glauconites in the layers Blue Earth, lower  
123 Blue Earth and lower Gestreifter Sand (Weitschat and Wichard 2010, Sadowski et al. 2017).  
124 The uncertainty range is due to a controversy over whether Baltic amber is autochthonously  
125 deposited in upper Eocene layers (Standke 1998, Sadowski et al. 2017), or redeposited there  
126 while originating from the Lower or Middle Eocene (Schulz 1999, Weitschat and Wichard  
127 2010). A recent study even suggests that Baltic amber was deposited in a periodic fashion  
128 between 45–35 Ma due to the transgression and regression of the sea into the amber-  
129 producing forests (Bukejs et al. 2019). Similarly controversial discussions are ongoing for the  
130 somewhat more precise age estimates of Rovno amber (37.8–33.9 Ma), with a trend in  
131 recent studies towards 37–35 Ma (Dunlop et al. 2019). Even though there is a possible  
132 overlap in the age estimates of Baltic and Rovno amber, Perkovsky et al. (2007) describe  
133 pronounced differences in their insect assemblages, which can be explained either by a  
134 different age, by the location on different land masses, or by different regional climatic  
135 conditions. The finding of a Pherhombinae rock fossil in the Fur Formation (earliest Eocene)  
136 could contribute as another piece of the puzzle to the discussion about the likely age of  
137 Baltic and Rovno ambers.

138  
139 *A combined approach to fossil placement*

140 To obtain a robust placement of the new fossil species among ichneumonid  
141 subfamilies, we combined morphometrics of the wing veins (Li et al. 2019) with a Bayesian  
142 phylogenetic analysis based on a dataset using both morphological and molecular data  
143 (Spasojevic et al. 2021). We also aimed to test Kasparyan's (1988, 1994) hypothesis about a  
144 close relationship of Pherhombinae with Townesitinae and Hybrizontinae using an extensive

145 taxon sampling and the addition of relevant morphological characters to a combined  
146 molecular and morphological matrix. In the light of our results, we describe the new fossil  
147 species in the genus *Pherhombus* and discuss the implications of this finding on the potential  
148 age of Baltic amber and on the quality of fossil placements based on combined Bayesian  
149 analyses.

150

## 151 **Materials and Methods**

### 152 *Morphological study of Fur fossil*

153 The studied rock fossil (FUR #10652) was found by Jan Verkleij in Ejerslev (Denmark)  
154 and is deposited at the Fur Museum in Nederby. Both part and counterpart were available  
155 and about equally informative. So far, no other specimens of this fossil species are known.  
156 Images of the dry fossil and of the fossil covered in 85% ethanol were made with the digital  
157 microscope *Keyence VHX 6000* at 200x magnification. Both stitching and stacking techniques  
158 were applied to enhance image quality. The interpretative line drawing was made with the  
159 open-source software GIMP. The drawing is based on both part and counterpart. Solid lines  
160 imply a higher certainty for the interpretation than dotted lines. Differences in line width are  
161 used to visualise larger and smaller structures and do not imply varying certainty.

162 Morphological terminology follows Broad et al. (2018), while abscissae of wing veins  
163 are denoted as in Spasojevic et al. (2018). The colour description is based on the colours  
164 visible in the fossil. The original colours of the species may differ from that.

165

### 166 *Morphometric analysis of wing venation*

167 After measuring several linear measurements that had been used in earlier studies of  
168 ichneumonid morphology (Bennett et al. 2019, Klopfstein and Spasojevic 2019), we chose  
169 the two most promising ratios to distinguish Mesochorinae and Pherhombinae based on  
170 visual inspection. For Mesochorinae, we obtained measurements from eight species based  
171 on drawings from Townes (1971) and for Pherhombinae, we used three wing photographs  
172 from Manukyan (2019), in combination with direct examination of two of the species. The  
173 new fossil species was measured from the obtained photographs, using average values from  
174 both forewings. To obtain an even denser taxon sampling, we in a second step also included  
175 incomplete fossils, for which only forewings could be measured, namely six fossil  
176 Mesochorinae (Brues 1910) and the three additional Pherhombinae species (Tolkanitz et al.  
177 2005, Manukyan 2019). For a complete list of taxa sampled and the data used from each,  
178 consider Supplementary File S1. Wing vein lengths were measured with ImageJ version 2.1.0  
179 and a scatterplot was obtained in R (R Core Team 2014).

180

### 181 *Morphological and molecular matrix*

182 To test alternative subfamily placements, we performed a Bayesian phylogenetic  
183 analysis based on a combined morphological and molecular matrix (Spasojevic et al. 2021)  
184 compiled for total-evidence dating (Pyron 2011, Ronquist et al. 2012a). To simplify and thus  
185 speed up the analysis, we only included one or two taxa from 31 of the 45 ichneumonid  
186 subfamilies (Supplementary File S1). For the two focal subfamilies, Mesochorinae and  
187 Pherhombinae, we increased the taxon sampling by newly coding the morphological  
188 characters and, for the former, complemented the dataset with sequence data for the genes  
189 28S and CO1 from Genbank (Table 1). In Mesochorinae, we coded one or two species in each  
190 extant genus, while we added all six described Pherhombinae species and a hitherto  
191 undescribed species from Baltic amber. To test the hypothesis that Pherhombinae are most  
192 closely related to Hybrizontinae and the extinct Townesitinae, we sampled additional species

193 from these two subfamilies (Table 1). We did not include the fossil Mesochorinae from  
194 Florissant Formation (Brues 1910) in the phylogenetic analysis, as their descriptions did not  
195 allow sufficient coding of morphological characters. However, we did include them in the  
196 morphometric analysis of the fore wing (see below).

197 Of the 222 characters coded in the morphological matrix by Spasojevic et al. (2021),  
198 we excluded 12 characters that either became uninformative under our restricted taxon  
199 sampling or consisted of large amounts of missing data and could in any case not be coded  
200 for fossils. The excluded characters are the following (numbering according to Spasojevic et  
201 al. 2021): #15 (Clypeus, apical tubercle: size); #33 (Occipital notch above foramen magnum:  
202 presence/absence); #34 (Foramen magnum, flange: width); #35 (Foramen magnum: shape);  
203 #36 (Foramen magnum: location); #91 (Intercoxal carinae, position); #92 (Hind coxa,  
204 apodeme: twisting); #93 (Propodeal denticles, presence/absence); #129 (Bullae in 2m-cu:  
205 size); #200 (Tergite 8 of female, lower anterolateral corner: shape); #203 (Tergites 8 & 9 in  
206 male: fusion); #207 (Tergite 9 in female: shape).

207  
208 [Table 1 around here]  
209

210 We added two characters that are informative about Mesochorinae and  
211 Pherhombinae: “Flagellomere 1: ratio of length to width” (continuous); and “Forewing vein  
212 1-M+1-Rs: length compared to length of r-rs” (continuous). In another two cases, we added  
213 states to existing characters in order to account for the newly included taxa: #133 (“Distal  
214 abscissa of Rs (4-Rs): shape”): (state 5) evenly arched towards 2-R1; #163 (“Tergite 1: shape  
215 from above”): (state 3) no clear separation of postpetiolus, constriction in the anterior half,  
216 thus expanding again towards the anterior margin. Sixteen characters were recorded as  
217 continuous characters and later on transformed to six-state, discrete characters in a linear  
218 fashion, as MrBayes only allows for a maximum of six states in ordered characters.

219 In the end, our matrix included 212 morphological characters from 12 fossil and 53  
220 extant species and molecular data from two to nine genes (4326 bp) from the latter. The  
221 molecular data was added to stabilize the backbone of the ichneumonid subfamily tree,  
222 given that previous analyses with morphological data only resulted in poor resolution of  
223 deeper nodes in the tree (Klopfstein and Spasojevic 2019). The dataset is available as  
224 Supplementary File S2 from the Dryad Digital Repository:

225 [https://doi.org/10.5061/dryad.\[NNNN\]](https://doi.org/10.5061/dryad.[NNNN]) and from TreeBASE under study TB2:S28484).

## 226 227 *Phylogenetic analysis*

228 A Bayesian analysis of the combined molecular and morphological partition was  
229 conducted in MrBayes 3.2 (Ronquist et al. 2012b). We used the Mkv model for the  
230 morphological partition (Lewis 2001), with 57 of the characters treated as ordered and rate-  
231 variation among characters modelled under a gamma distribution. This model was preferred  
232 over an unordered or an equal-rates model in analyses of a precursor dataset (Klopfstein  
233 and Spasojevic 2019). The molecular data was partitioned as in Spasojevic et al. (2021) and  
234 analysed under a reversible-jump MCMC substitution model (Huelsenbeck et al. 2004),  
235 including a gamma-distribution and invariant sites to model among-site rate variation.

236 Four independent runs of four Metropolis-coupled chains each were run for 100  
237 million generations and convergence was assessed by inspection of the likelihood plots,  
238 effective sample sizes, potential scale-reduction factors and average standard deviation of  
239 split frequencies (ASDSF). Convergence was difficult to attain, especially on topology, with  
240 ASDSF values among the four independent runs not dropping below 0.029. This was

241 probably due to the fossils acting as rogue taxa, a suspicion that was confirmed when  
242 comparing consensus trees with fossils included or excluded. We thus also constructed  
243 consensus trees for each of the four runs independently to make sure that our results were  
244 not influenced unduly by different runs getting stuck on different topology islands. We  
245 conservatively excluded the first half of each run as burn-in. The tree was rooted with  
246 Xoridinae as outgroup, as suggested by recent phylogenetic analyses (Bennett et al. 2019,  
247 Klopfstein et al. 2019a).

248

#### 249 *Rogue Plots*

250 To calculate and illustrate alternative placements of our fossil, we constructed  
251 RoguePlots (Klopfstein and Spasojevic 2019). To that end, we sampled 1000 evenly spaced  
252 trees from the post-burn-in period of all four MCMC runs in the Bayesian analysis, both  
253 separately and combined, using a custom bash script. These trees were input into the  
254 `create.rogue.plot` function in the `rogue.plot` package in R (R Core Team 2014), together with  
255 the consensus tree of all the other taxa, excluding the fossil in question.

256

### 257 **Results**

#### 258 *Morphometric Analysis*

259 Both studied wing venation ratios clearly indicate that the new fossil species belongs  
260 to the subfamily Pherhombinae rather than Mesochorinae (Fig. 1), with both ratios allowing  
261 for a clear separation of the two subfamilies. This finding is robust to the addition of  
262 forewing information of the remaining, incomplete Pherhombinae and Mesochorinae fossils  
263 (Supplementary File S3).

264

265 [Figure 1 around here]

266

#### 267 *Phylogeny and Rogue Plot*

268 The phylogenetic and RoguePlot analyses undoubtedly assign the new fossil species  
269 to Pherhombinae (Fig. 2), with 1.0 posterior probability in each of the four independent  
270 MCMC runs, while there was zero support for an alternative placement with Mesochorinae.  
271 With a posterior probability of 0.64 (0.625 to 0.668 in the four runs), the new species is  
272 placed as the sister taxon to the other *Pherhombus* species. The remaining 0.36 probability is  
273 distributed to branches within the clade formed by the other *Pherhombus* species.  
274 Furthermore, the main subfamily clades (Ichneumoniformes, Pimpliformes and  
275 Ophioniformes) were all recovered in the analysis, although sometimes with low support  
276 (Fig. 2). As suggested earlier, Pherhombinae are placed in a clade with Hybrizontinae and  
277 Townesitinae within the higher Ophioniformes. Support is surprisingly high for a sister  
278 relationship between Pherhombinae and Hybrizontinae, given that the former only had  
279 morphological data (pp = 0.87). The clade in which these two group with Townesitinae is  
280 somewhat less well supported (pp = 0.62), as is their placement among the higher  
281 ophioniform subfamilies (Anomaloninae, Campopleginae, Cremastinae, Ophioninae; pp =  
282 0.64). These results were consistent across all four independent runs.

283

284 [Figure 2 around here]

285

286

287

288

289 *Systematic Palaeontology*

290

291 Family Ichneumonidae Latreille, 1802

292 Subfamily Pherhombinae Kasparyan, 1988

293 Genus *Pherhombus* Kasparyan, 1988

294 *Pherhombus parvulus* n. sp.

295 Figure 3

296 **Material.** Holotype, #10652, part and counterpart; sex unknown. Part and counterpart  
297 about equally informative, often showing complementary structures (e.g. first tergite).  
298 Collector: Jan Verkleij. Deposited at Fur Museum, Nederby.

299 **Type horizon and locality.** The fossil was found in Denmark, Morsø Kommune, Ejerslev  
300 in cement stone which has a geological age of about 54 Ma (early Eocene).

301 **Etymology.** In latin, “parvulus” is the diminutive of “parvus” which means small or tiny.  
302 This refers to the fact that the fossil species is only 3.3 mm long, which is about half the size  
303 of all other described Pherhombinae.

304 **Diagnosis.**

305 **Taxonomic placement.** Due to the nearly complete preservation of the forewing  
306 venation, this species can be placed within the Ichneumonidae with certainty, which are  
307 distinguished from the related Braconidae by lacking vein 1-Rs+M (sometimes with the  
308 exception of a short remain, called ramulus) and by the presence of 2m-cu. The rhombic  
309 aerolet is the probably most conspicuous character visible in this fossil; it is only shared by  
310 members of the subfamilies Mesochorinae and Pherhombinae. Several characters, such as  
311 the low number of antennal segments, the forewing 1-M+1-Rs to r-rs ratio, the hindwing 1-  
312 Rs to rs-m ratio and the elongated and parallel-sided first tergite give evidence for the  
313 placement within the monotypic Pherhombinae. Even though the new species was placed  
314 with the highest probability as a stem representative, there is currently not sufficient  
315 morphological evidence that this species should be placed within a new genus. This  
316 placement is supported both by the morphometric and Bayesian phylogenetic analyses (Figs  
317 1 and 2).

318 **Species diagnosis.** This species is very similar both in wing venation and shape of the  
319 first tergite to many species of *Pherhombus*. Nevertheless, it can be easily distinguished from  
320 all currently described species by its small size (body length: 3.3 mm, forewing length: 2.9  
321 mm), with all other *Pherhombus* species ranging in body length from 6.7 to more than 9 mm  
322 and forewing length from 4.7 to 9.5 mm (Tolkanitz et al. 2005, Manukyan 2019). It is further  
323 distinguished from most other species by the parallel-sided antennal segments, which are  
324 otherwise widened towards the apex in all species except perhaps *P. kraxtepellensis* and *P.*  
325 *kasparyani* (Manukyan, 2019), whose antennae are widest around the 8<sup>th</sup> or 9<sup>th</sup> flagellomere  
326 and only slightly expanded apically. The new species can be distinguished from these two by  
327 the presence of a distinct ramulus and by the hyaline wings (smoky in *P. kasparyani*).

328 **Description.**

329 **Preservation.** Dorsal view. Head only partially preserved, antennae nearly complete  
330 with partly clear segmentation. Mesosoma not well preserved, hardly any characters visible  
331 except possible hind border of mesoscutum; wings stretched out flat, all four wings nearly  
332 complete; partial mid and hind legs visible. Metasoma anteriorly almost complete but  
333 segmentation posteriorly unclear; posterior part of metasoma ending abruptly or  
334 incomplete, genitalia not visible.

335 Body 3.3 mm; fossil in different shades of brown; strongly sclerotized parts, such as  
336 head or first tergite, distinctly darker than rest, wings hyaline.

337        *Head* deformed, no detailed structures distinguishable. Antenna slender, with about  
338        20 flagellomeres (+/- 3); scape and pedicel of normal dimensions (as far as visible), first  
339        flagellomere almost 7.0 times longer than apically wide.

340        *Mesosoma* rather short and stout; triangular dark patches at forewing base probably  
341        corresponding to axial sclerites. Forewing 2.9 mm; areolet closed, rhombic, 3r-m with a bulla  
342        at posterior end; 4-Rs straight; ramulus present, slightly longer than width of surrounding  
343        veins; pterostigma 4.5 x longer than wide; radial cell 3 x longer than wide; 1cu-a meeting  
344        M+Cu opposite 1-M&1-RS; 2m-cu nearly straight, somewhat inclivous, probably with a single  
345        large bulla in anterior third or half; 3-Cu about 0.75 x as long as 2cu-a. Hindwing 1-Rs 0.47 x  
346        as long as rs-m; 2-Rs tubular on entire length (not counting last 10%); 1-Cu clearly shorter  
347        than cu-a. Mid leg very slender, both coxa, femur and parts of tibia and tarsus visible. Hind  
348        leg with very long coxa, at least 2.1 x longer than wide; both femur and parts of tibia  
349        preserved, femur rather elongated, more than 5.0 x longer than wide.

350        *Metasoma* appearing somewhat club-shaped, with widest part close to posterior end;  
351        tergite 1 slightly more than 4 x longer than wide, narrow and parallel sided; tergite 2  
352        transverse, 0.75 x as long as wide. Posterior metasomal segments appear truncated, lack of  
353        ovipositor suggests a male, but incomplete preservation also possible.

354

355        [Figure 3 around here]

356

357

## 358        **Discussion**

### 359        *Integrative analysis facilitates firm fossil placement*

360        The integrative approach we followed here facilitated a firm placement of the newly  
361        described fossil species in an extinct subfamily. The discussion whether to work with  
362        molecular or morphological data is omnipresent in entomological systematics. In most cases,  
363        integrative approaches are beneficial for taxonomic studies as they manage to grasp more of  
364        the available information (Schlick-Steiner et al. 2010, Yeates et al. 2011, Wang et al. 2015,  
365        Gokhman 2018). This is just as true for the phylogenetic placement of fossils –  
366        complementing morphological analyses with molecular data for recent taxa gives higher  
367        stability especially to the backbone of phylogenetic trees (Nylander et al. 2004, Ronquist et  
368        al. 2012a, Spasojevic et al. 2021). However, placement of fossils is only possible if extensive  
369        morphological data is included for extant taxa as well, because extant taxa with missing  
370        morphological information can attract fossils in phylogenetic analyses (Spasojevic et al.  
371        2021). Thus, morphological data should be coded for all included extant taxa, which proved  
372        to be a powerful approach in our study.

373        A potential drawback of Bayesian phylogenetic inference is the difficulty to directly  
374        assess the impact of individual characters on the outcome. To make sure that an analysis  
375        was not biased by few characters, several steps are possible. Character state changes can be  
376        mapped onto a phylogeny, characters can be excluded in the analysis in order to check for  
377        their impact, or additional analyses based on only a few characters can be conducted to  
378        assess their respective signal. In our case, we separately analysed morphometric data on  
379        wing venation of Pherhombinae and Mesochorinae and thus identified two ratios with high  
380        information content with regard to the differentiation of these two groups. With very few  
381        exceptions, wing venation characters have not received much attention in subfamily  
382        identification in Ichneumonidae (Broad et al. 2018, but see Li et al. 2019), and our results  
383        suggest that they should be explored in more detail in the future, maybe even in the  
384        framework of geometric morphometrics.

385 Not only an overrated single character, but also a systematic bias could alter the  
386 result of the analysis. In the study at hand, a potential source of systematic bias is body size,  
387 which often influences several traits at once (Minelli and Fusco 2019). Miniaturisation  
388 effects often include parallel character loss, morphological simplification, and allometric  
389 effects that might change morphometric ratios (Gould 1966, Klopstein et al. 2015, Knauthe  
390 et al. 2016). Therefore, *P. parvulus* could have been placed in the clade of Pherombinae,  
391 Townesitinae and Hybrizontinae because all of them are rather small ichneumonids. Indeed,  
392 some of the character states that support this placement might be related to a reduction in  
393 size, for example the reduced number of palpal segments and reduced mandibles. However,  
394 other characters are less likely to be a result of miniaturization, such as the elongate hind  
395 coxae or shape of first tergite (for more characters, see next section). Also, we found that  
396 the wing vein ratios of the new species are very similar to those of the other *Pherhombus*  
397 species, even though these are distinctly larger in body size. Furthermore, other subfamilies  
398 with many small-bodied taxa (e.g. Orthocentrinae, Phygadeuontinae, Campopleginae) did  
399 not attract the new fossil species at all (Fig. 2). We thus consider the placement as reliable,  
400 even though further research is needed to support the close relationship between the three  
401 subfamilies.

402 Another possible source of systematic bias is the heterogeneous origin of  
403 morphological data used in this study. Some extant taxa were studied directly and thus with  
404 detailed morphological data, some were coded based only on drawings and descriptive texts  
405 (Townes 1971). Most amber fossils that we studied were well preserved and thus show  
406 rather complete coding, often approaching extant taxa with respect to completeness (Table  
407 1); but only a few characters could be coded for the new rock fossil species. Previous studies  
408 using the total-evidence dating framework and thus working with similarly incomplete data  
409 matrices found that even poorly coded fossils can contribute considerably to an analysis,  
410 while missing data did not seem to negatively affect the outcome (Ronquist et al. 2012a).  
411 Similarly, we here found no evidence that heterogeneous completeness biased the  
412 phylogenetic analysis, since even subfamilies which included species from very different data  
413 sources were retrieved with high support, and the new rock fossil species was placed very  
414 confidently with the amber Pherombinae in the phylogenetic tree.

415 Resolution of the phylogeny reconstructed here is rather high, considering that  
416 inference of considerable portions of the tree were only informed by morphology, especially  
417 in the extinct Pherombinae and Townesitinae. The analysis of morphological characters in a  
418 phylogenetic context of course always relies to a certain extent on the availability of an  
419 appropriate model of character evolution (Lewis 2001, Klopstein et al. 2015, Wright et al.  
420 2016). However, the high congruence between the morphological and molecular partition in  
421 our dataset suggests that model mismatch is not strongly misleading our results (Klopstein  
422 and Spasojevic 2019), although our analysis would certainly profit from the development of  
423 more refined models of morphological evolution.

#### 424 425 *Phylogenetic support for Kasparyan's hypothesis*

426 Our phylogenetic analysis supports Kasparyan's hypothesis (1988, Kasparyan 1994)  
427 that Pherombinae, Townesitinae and Hybrizontinae form a clade, which in our analysis was  
428 located within the higher Ophioniformes. The three subfamilies share several derived  
429 character states from different parts of the body, though most of them are not entirely  
430 exclusive to the three. The strongly convex clypeus also occurs in Orthocentrinae, an extant  
431 subfamily that consists exclusively of small-bodied taxa. However, it is less convex in  
432 Orthocentrinae and much more narrow in Hybrizontinae than in the other subfamilies. The

433 maxillary and labial palps have a reduced number of segments in Hybrizontinae,  
434 Pherombinae and in one of the two tribes of Townesitinae, but not in Orthocentrinae. Vein  
435 r-rs in the forewing is conspicuously shortened in all three subfamilies, as is 1RS in the  
436 hindwing in those species where it is visible (Fig. 1). The hind coxa is rather elongate, and the  
437 first tergite is narrow and elongate in all three subfamilies, although more strongly so in  
438 Pherombinae.

439 In our tree, Hybrizontinae and Pherombinae group together, which was also  
440 Kasparyan's initial suggestion (1988). Later, he apparently changed his mind, assuming that  
441 Pherombinae and Townesitinae were more closely related (Kasparyan 1994, Manukyan  
442 2019), which was also the outcome of a previous phylogenetic study with a more sparse  
443 taxon sampling (Spasojevic et al. 2021). Our current analysis now once more revives the  
444 initial suggestion of close ties between Pherombinae and the highly derived Hybrizontinae,  
445 and several character states support this relationship. The mandibles are reduced to a flap-  
446 like structure in Hybrizontinae, Pherombinae and in some species of *Orthocentrus*, while  
447 being complete with two teeth in Townesitinae. The metasomal cavity is moved upwards  
448 with respect to the metacoxal cavities in both Pherombinae and Hybrizontinae, but not  
449 Townesitinae, a state that is otherwise only present in Labeninae. Finally, the hind coxa is  
450 much more strongly elongate in Pherombinae and Hybrizontinae than in Townesitinae.

451 Based on Kasparyan's (1994) suggested relationships, Manukyan (2019) inferred that  
452 the three subfamilies have split in the mid to late Eocene. Considering that the new fossil  
453 species is clearly placed after the splitting of Pherombinae and Hybrizontinae and given the  
454 age of the Fur Formation, we can provide good evidence that the last common ancestor of  
455 the three groups lived much earlier than that, probably already in the Palaeocene or earlier.  
456 This suggestion is supported by the outcome of a recent dating analysis, which found that  
457 most subfamilies of Darwin wasps already diversified in the Mesozoic (Spasojevic et al.  
458 2021). Studies of late Cretaceous ambers should thus consider the possibility that members  
459 of these subfamilies or stem-lineages there-of already occurred before the K-Pg mass  
460 extinction.

461  
462 *Presence of Pherombinae in rock deposit from earliest Eocene*

463 Defining the age span of the monotypic Pherombinae is rather difficult because up  
464 to now, only amber fossil species were known. *Pherombus dolini* from Rovno amber  
465 (Tolkanitz et al. 2005) anchors the upper age limit of the subfamily in the upper Eocene  
466 (33.9–37.8 Ma). The other *Pherombus* species are known only from Baltic amber and thus  
467 do not provide much information about the age span of Pherombinae, as the age of Baltic  
468 amber is still highly controversial in the paleontological community (Standke 1998, Schulz  
469 1999, Weitschat and Wichard 2010, Sadowski et al. 2017, Tolkanitz and Perkovsky 2018).  
470 Our finding of *P. parvulus* from a lowermost Eocene rock deposit pushes back the lower age  
471 maximum of *Pherombus* to about 54 Ma, thus leading to a minimal age span of the  
472 subfamily of nearly 20 million years. Even though this is a long time period, it should not be  
473 considered as unlikely, given that other ichneumonid genera existed for much longer  
474 periods, e.g., *Phaenolobus* or *Xanthopimpla* (56 and 54 Ma–present: Piton 1940, Klopstein  
475 in press). Considering these long time windows for ichneumonid genera, making inferences  
476 from *P. parvulus* on the age estimate of Baltic amber appears unwarranted; however, its  
477 finding at least allows for the possibility that Baltic amber might be considerably older than  
478 Rovno amber. On the other hand, our phylogenetic analysis suggests that *P. parvulus* is the  
479 sister taxon to all other *Pherombus* species, which is congruent with the notion that it lived  
480 much earlier than its congeners. Interestingly, our new species is not just the oldest but also

481 the smallest species known of this subfamily, which is remarkable given that it was found in  
482 rock rather than amber, even though the latter is typically known for a bias towards small-  
483 bodied taxa. This might indicate that Pherhombinae increased their body size over time,  
484 even though this conclusion is somewhat shaky given the low number of known species.

485 The new Pherhombinae fossil described here exemplifies just how poorly studied  
486 ichneumonid fossils still are. Future studies might reveal an even more extensive temporal  
487 distribution of this enigmatic subfamily and might provide further clues as to their ecology  
488 and evolution. Furthermore, each described and properly placed fossil Darwin wasp can  
489 contribute to the proper calibration of the phylogenetic tree of this hyperdiverse insect  
490 group and thereby improve our knowledge of its evolution and diversification.

491

## 492 **Funding**

493 This study was supported by the Swiss National Science Foundation (grant  
494 310030\_192544).

495

## 496 **Acknowledgements**

497 We are grateful to René Sylvestersen of the Fur Museum in Nederby, Denmark, for  
498 providing the fossil described here. We thank Lars Vilhelmsen (Natural History Museum of  
499 Denmark, Copenhagen), Dmitry Kopylov (Paleontological Institute, Russian Academy of  
500 Sciences, Moscow, Russia) and Michael Rasser (Staatliches Museum für Naturkunde  
501 Stuttgart, Germany) for access to amber fossils from their collections for comparison.  
502 Tamara Spasojevic and Bastien Mennecart provided valuable feedback on an earlier version  
503 of the manuscript.

504 Computations were performed on the HPC cluster UBELIX of the University of Bern,  
505 Switzerland (<http://www.id.unibe.ch/hpc>).

506

## 507 **Data availability**

508 All data used in this study is available from the Dryad Digital Repository:

509 [https://doi.org/10.5061/dryad.\[NNNN\]](https://doi.org/10.5061/dryad.[NNNN])

510

## 511 **References**

512 Ansorge J. 1993. Schlupfwespen aus dem Moler Dänemarks – ein aktualistischer Vergleich. Fossilien.  
513 Korb, Goldschneck-Verlag, p. 111-113.

514 Belshaw R, Grafen A, Quicke DLJ. 2003. Inferring life history from ovipositor morphology in parasitoid  
515 wasps using phylogenetic regression and discriminant analysis. Zool J Linn Soc, 139:213-228  
516 doi: <https://doi.org/10.1046/j.1096-3642.2003.00078.x>.

517 Bennett AMR, Cardinal S, Gauld ID, Wahl DB. 2019. Phylogeny of the subfamilies of Ichneumonidae  
518 (Hymenoptera). J Hym Res, 71:1–156 doi: <https://doi.org/10.3897/jhr.71.32375>.

519 Broad GR, Shaw MR, Fitton MG. 2018. Ichneumonid wasps (Hymenoptera: Ichneumonidae): their  
520 classification and biology. Handbooks for the identification of British insects, 7:1-418.

521 Brues CT. 1910. The parasitic Hymenoptera of the Tertiary of Florissant, Colorado. Bulletin of the  
522 Museum of Comparative Zoology at Harvard University, 54:1-125.

523 Brues CT. 1923. Some new fossil parasitic Hymenoptera from Baltic amber. Proceedings of the  
524 American Academy of Arts and Sciences, 58:327–346 doi: <https://doi.org/10.2307/20025999>.

525 Bukejs A, Alekseev VI, Pollock DD. 2019. Waidelotinae, a new subfamily of Pyrochroidae (Coleoptera:  
526 Tenebrionoidea) from Baltic amber of the Sambian peninsula and the interpretation of  
527 Sambian amber stratigraphy, age and location. Zootaxa, 4664:261–273 doi:  
528 <https://doi.org/10.11164/zootaxa.4664.2.8>.

529 Chambers LM, Pringle M, Fitton G, Larsen LM, Pedersen AK, Parrish R. 2003. Recalibration of the  
530 Palaeocene-Eocene boundary (PE) using high precision U-Pb and Ar-Ar isotopic dating. EGS-  
531 AGU-EUG Joint Assembly. Nice.

532 Dunlop JA, Vlaskin AP, Marusik Y. 2019. Comparing arachnids in Rovno amber with the Baltic and  
533 Bitterfeld deposits. *Paleontological Journal*, 53:92–101 doi:  
534 <https://doi.org/10.1134/S0031030119100034>.

535 Forbes AA, Bagley RK, Beer MA, Hippee AC, Widmayer HA. 2018. Quantifying the unquantifiable: why  
536 Hymenoptera – not Coleoptera – is the most speciose animal order. *BMC Ecology*, 18:21 doi:  
537 <https://doi.org/10.1186/s12898-018-0176-x>.

538 Gokhman VE. 2018. Integrative taxonomy and its implications for species-level systematics of  
539 parasitoid Hymenoptera. *Entomological Review*, 98:834–864 doi:  
540 <https://doi.org/10.1134/S0013873818070059>.

541 Gould SJ. 1966. Allometry and size in ontogeny and phylogeny. *Biol Rev*, 41:587–640 doi:  
542 <https://doi.org/10.1111/j.1469-185X.1966.tb01624.x>.

543 Henriksen KL. 1922. Eocene insects from Denmark. *Danmarks geologiske Undersøgelse*, 2:1-36 doi:  
544 <https://doi.org/10.34194/raekke2.v37.6823>.

545 Huelsenbeck JP, Larget B, Alfaro ME. 2004. Bayesian phylogenetic model selection using reversible-  
546 jump Markov chain Monte Carlo. *Mol Biol Evol*, 21:1123-1133 doi:  
547 <https://doi.org/10.1093/molbev/msh123>.

548 Kasparyan DR. 1988. A new subfamily and two new genera of ichneumonids (Hymenoptera,  
549 Ichneumonidae) from Baltic amber. [In Russian]. *Proceedings of the Zoological Institute*  
550 Leningrad, 175:38-42.

551 Kasparyan DR. 1994. A review of the Ichneumon flies of Townesitinae subfam. nov. (Hymenoptera,  
552 Ichneumonidae) from the Baltic amber. *Paleontological Journal*, 28:114–126.

553 Klopfstein S. in press. High diversity of pimpline parasitoid wasps (Hymenoptera, Ichneumonidae,  
554 Pimplinae) in the Fur Formation in Denmark. *Geodiversitas*.

555 Klopfstein S, Langille B, Spasojevic T, Broad GR, Cooper SJB, Austin AD, Niehuis O. 2019a. Hybrid  
556 capture data unravels a rapid radiation of pimpliform parasitoid wasps (Hymenoptera:  
557 Ichneumonidae: Pimpliformes). *Syst Entomol*, 44:361-383 doi:  
558 <https://doi.org/10.1111/syen.12333>.

559 Klopfstein S, Santos B, Shaw MR, Alvarado M, Bennett AMR, Dal Pos D, Giannotta M, Herrera Florez  
560 AF, Karlsson D, Khalaim AI, et al. 2019b. Darwin wasps: a new name heralds renewed efforts to  
561 unravel the evolutionary history of Ichneumonidae. *Entomological Communications*,  
562 1:ec01006 doi: <https://doi.org/10.37486/2675-1305.ec01006>.

563 Klopfstein S, Spasojevic T. 2019. Illustrating phylogenetic placement of fossils using RoguePlots: An  
564 example from ichneumonid parasitoid wasps (Hymenoptera, Ichneumonidae) and an extensive  
565 morphological matrix. *PLoS One*, 14:e0212942 doi:  
566 <https://doi.org/10.1371/journal.pone.0212942>.

567 Klopfstein S, Vilhelmsen L, Ronquist F. 2015. A nonstationary Markov model detects directional  
568 evolution in hymenopteran morphology. *Syst Biol*, 64:1089–1103 doi:  
569 <https://doi.org/10.1093/sysbio/syv052>.

570 Knauthe P, Beutel RG, Hörnschemeyer T, Pohl H. 2016. Serial block-face scanning electron  
571 microscopy sheds new light on the head anatomy of an extremely miniaturized insect larva  
572 (Insecta, Strepsiptera). *Arthropod Syst Phylogeny*, 74:107–126.

573 Larsson SG. 1975. Palaeobiology and mode of burial of the insects of the lower Eocene Mo-clay of  
574 Denmark. *Bulletin fo the geological society of Denmark*, 24:193-209.

575 Lewis PO. 2001. A likelihood approach to estimating phylogeny from discrete morphological  
576 character data. *Syst Biol*, 50:913-925 doi: <https://doi.org/10.1080/106351501753462876>.

577 Li L, Shih PJM, Kopylov DS, Li D, Ren D. 2019. Geometric morphometric analysis of Ichneumonidae  
578 (Hymenoptera: Apocrita) with two new Mesozoic taxa from Myanmar and China. *Journal of*  
579 *Systematic Palaeontology*, DOI: 10.1080/14772019.2019.1697903 doi:  
580 <https://doi.org/10.1080/14772019.2019.1697903>.

581 Manukyan AR. 2019. New data on ichneumon wasps of the subfamily Pherhombinae (Hymenoptera,  
582 Ichneumonidae) from Baltic amber, with descriptions of three new species. *Entomological  
583 Review*, 99:1324–1338 doi: <https://doi.org/10.1134/S0013873819090112>.

584 McIntosh WC, Geissmann JW, Chapin CE, Kunk MJ, Henry CD. 1992. Calibration of the latest Eocene-  
585 Oligocene geomagnetic polarity time scale using  $^{40}\text{Ar}/^{39}\text{Ar}$  dated ignimbrites. *Geology*,  
586 20:459–463 doi: [https://doi.org/10.1130/0091-7613\(1992\)020<0459:COTLEO>2.3.CO;2](https://doi.org/10.1130/0091-7613(1992)020<0459:COTLEO>2.3.CO;2).

587 Minelli A, Fusco G. 2019. No limits: Breaking constraints in insect minituarization. *Arthropod Struct  
588 Dev*, 48:4-11 doi: <https://doi.org/10.1016/j.asd.2018.11.009>.

589 Nylander JAA, Ronquist F, Huelsenbeck JP, Nieves-Aldrey JL. 2004. Bayesian phylogenetic analysis of  
590 combined data. *Syst Biol*, 53:47–67 doi: <https://doi.org/10.1080/10635150490264699>.

591 Perkovsky EE, Rasnitsyn AP, Vlaskin AP, Taraschuk MV. 2007. A comparative analysis of the Baltic and  
592 Rovno amber arthropod faunas: representative samples. *African Invertebrates*, 48:229–245  
593 doi: [10.10520/EJC84578](https://doi.org/10.10520/EJC84578).

594 Piton L. 1940. Paléontologie du gisement éocène de Menat (Puy-de-Dôme) (Flore et Faune). Faculté  
595 des Sciences. Clermont-Ferrand, Université de Clermont p. 303.

596 Pyron RA. 2011. Divergence time estimation using fossils as terminal taxa and the origins of  
597 Lissamphibia. *Syst Biol*, 60:466-481.

598 R Core Team. 2014. R: A language and environment for statistical computing. Vienna, Austria, R  
599 Foundation for Statistical Computing.

600 Ritzkowski S. 1997. K-Ar-Altersbestimmungen der bernsteinführenden Sedimente des Samlandes  
601 (Paläogen, Bezirk Kaliningrad). *Metalla*, Bochum, 66:19–23.

602 Ronquist F, Forshage M, Häggqvist S, Karlsson D, Hovmöller R, Bergsten J, Holston K, Britton T,  
603 Abenius J, Andersson B, *et al.* 2020. Completing Linnaeus's inventory of the Swedish insect  
604 fauna: Only 5,000 species left? *PLoS One*, 15:e0228561 doi:  
605 <https://doi.org/10.1371/journal.pone.0228561>.

606 Ronquist F, Klopfstein S, Vilhelmsen L, Schulmeister S, Murray DL, Rasnitsyn AP. 2012a. A total-  
607 evidence approach to dating with fossils, applied to the early radiation of the Hymenoptera.  
608 *Syst Biol*, 61:973–999 doi: <http://dx.doi.org/10.1093/sysbio/sys058>.

609 Ronquist F, Teslenko M, Van der Mark P, Ayres DL, Darling A, Höhna S, Larget B, Liu L, Suchard MA,  
610 Huelsenbeck JP. 2012b. MrBayes 3.2: Efficient Bayesian phylogenetic inference and model  
611 choice across a large model space. *Syst Biol*, 61:539–542 doi:  
612 <https://doi.org/10.1093/sysbio/sys029>.

613 Rust J. 1998. Biostratinomie von Insekten aus der Fur-Formation von Dänemark (Moler, oberes  
614 Paleozän / unteres Eozän). *Paläontologische Zeitschrift*, 72:41-58 doi:  
615 <https://doi.org/10.1007/BF02987814>.

616 Rust J. 2000. Fossil record of mass moth migration. *Nature*, 405:530-531 doi:  
617 <https://doi.org/10.1038/35014733>.

618 Sadowski EM, Schmidt AR, Saeyfullah LJ, Kunzmann L. 2017. Conifers of the 'Baltic amber forest' and  
619 their palaeoecological significance. *Stapfia*, 106:2–73.

620 Schlick-Steiner BC, Steiner FM, Seifert B, Stauffer C, Christian E, Crozier RH. 2010. Integrative  
621 taxonomy: a multisource approach to exploring biodiversity. *Annu Rev Entomol*, 55:421-438  
622 doi: <https://doi.org/10.1146/annurev-ento-112408-085432>.

623 Schulz W. 1999. The Baltic Amber in Quaternary sediments, a review of its occurrence, the largest  
624 specimens and amber museums. *Archiv für Geschiebekunde*, 2:459-478.

625 Spasojevic T, Broad GR, Bennett AMR, Klopfstein S. 2018. Ichneumonid parasitoid wasps from the  
626 Early Eocene Green River Formation: five new species and a revision of the known fauna  
627 (Hymenoptera, Ichneumonidae). *Paläontologische Zeitschrift*, 92:35-63 doi:  
628 <https://doi.org/10.1007/s12542-017-0365-5>.

629 Spasojevic T, Broad GR, Sääksjärvi IE, Schwarz M, Ito M, Matsumoto R, Hopkins T, Klopfstein S. 2021.  
630 Mind the outgroup and bare branches in total-evidence dating: a case study of pimpliform  
631 Darwin wasps (Hymenoptera, Ichneumonidae). *Syst Biol*, 70:322-339 doi:  
632 <https://doi.org/10.1093/sysbio/syaa079>.

633 Standke G. 1998. Die Tertiärprofile der Sammländischen Bernsteinküste bei Rauschen. Schriftenreihe  
634 für Geowissenschaften, 7:93–133.

635 Tolkanitz VI, Narolsky NB, Perkovsky EE. 2005. A new species of parasite wasp of the genus  
636 *Pherhombus* (Hymenoptera, Ichneumonidae, Pherhombinae) from the Rovno Amber [in  
637 Russian]. Paleontologicheskii Zhurnal, 5:50–52.

638 Tolkanitz VI, Perkovsky EE. 2018. First record of the late Eocene Ichneumon fly *Rasnitsynites tarsalis*  
639 Kasparyan (Ichneumonidae, Townesitinae) in Ukraine confirms correlation of the upper Eocene  
640 Lagerstätten. Paleontological Journal, 52:31–34 doi:  
641 <https://doi.org/10.1134/S0031030118010136>.

642 Townes HK. 1971. The genera of Ichneumonidae, Part 4. Memoirs of the American Entomological  
643 Institute, 17:1-372.

644 Wang Y, Nansen C, Zhang Y. 2015. Integrative insect taxonomy based on morphology, mitochondrial  
645 DNA, and hyperspectral reflectance profiling. Zool J Linn Soc, 177:378–394 doi:  
646 <https://doi.org/10.1111/zoj.12367>.

647 Weitschat W, Wichard W. 2010. Baltic Amber. In: Penney D editor. Biodiversity of fossils in amber  
648 from the major world deposits. Manchester, Siri Scientific Press, p. 80-115.

649 Westerhold T, Röhl U, McCarren HK, Zachos JC. 2009. Latest on the absolute age of the  
650 Paleocene–Eocene Thermal Maximum (PETM): New insights from exact stratigraphic position  
651 of the key ash layers +19 and –17. Earth and Planetary Science Letters, 287:412-419 doi:  
652 <https://doi.org/10.1016/j.epsl.2009.08.027>.

653 Wright AM, Lloyd GT, Hillis DM. 2016. Modeling character change heterogeneity in phylogenetic  
654 analyses of morphology through the use of priors. Syst Biol, 65:602-611 doi:  
655 <https://doi.org/10.1093/sysbio/syv122>.

656 Yeates DK, Seago A, Nelson L, Cameron SL, Joseph L, Trueman JWH. 2011. Integrative taxonomy, or  
657 iterative taxonomy? Syst Entomol, 36:209–217.

658 Yu DS, Van Achterberg C, Horstmann K. 2016. Taxapad 2016. Ichneumonoidea 2015 (Biological and  
659 taxonomical information), Taxapad Interactive Catalogue Database on flash-drive. Nepean,  
660 Ottawa, Canada, [www.taxapad.com](http://www.taxapad.com).

661

662

663 **Tables**

664

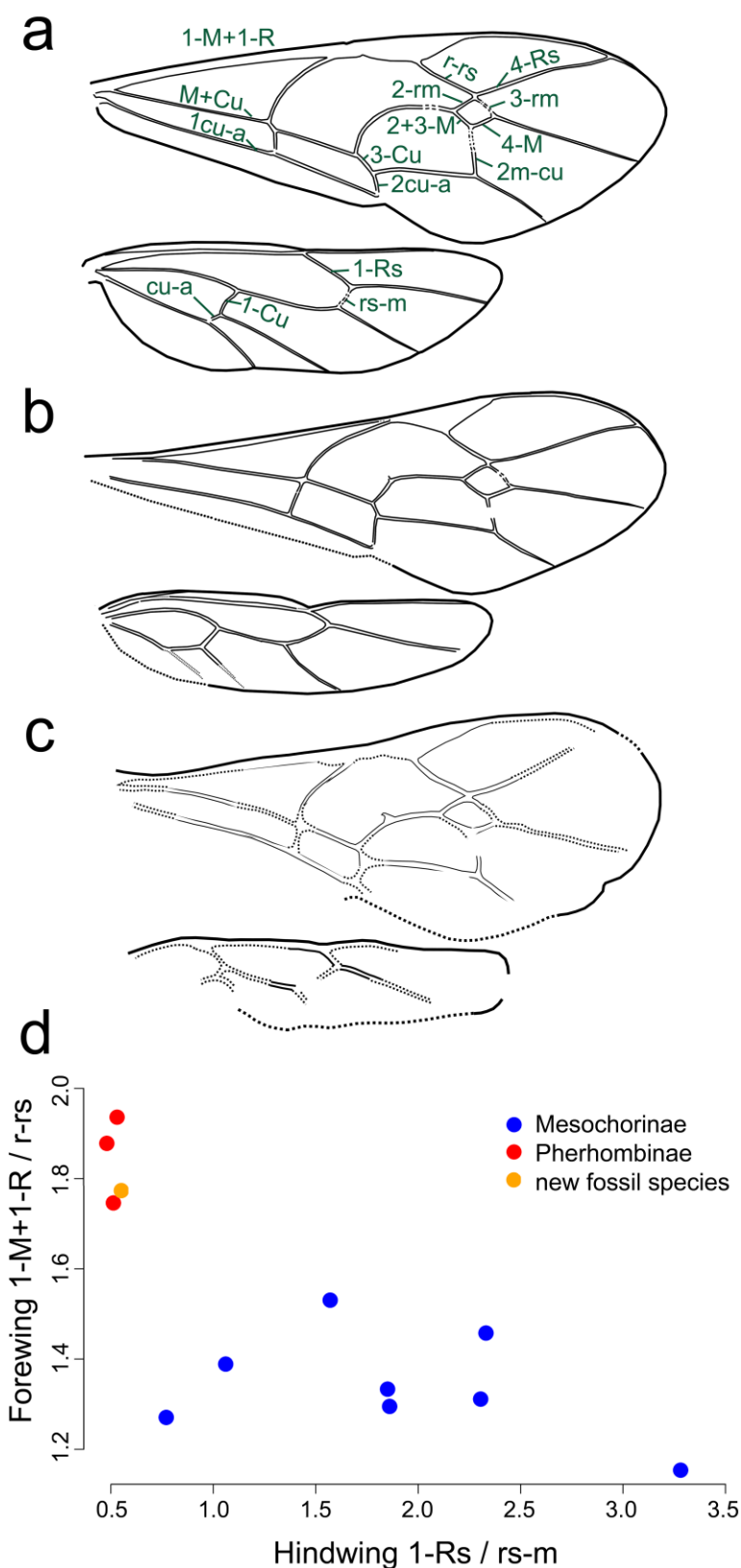
Table 1. Added taxa or taxa with expanded morphological coding in comparison to the dataset from Spasojevic et al. (2021).

Subfamily	Genus	species	ID or provenience <sup>1</sup>	coding completeness	extant / fossil: Formation	Genbank 28S/CO1
Hybrizontinae	<sup>2</sup> <i>Tobiasites</i>	<i>striatus</i>	NHMD 876107		fossil: Baltic	
Mesochorinae	<i>Astiphromma</i>	<i>albitarsis</i>	LIT: Townes 1969	63%	amber	
Mesochorinae	<i>Cidaphus</i>	<i>atricilla</i>	NMB: #2603	81%	extant	
Mesochorinae	<i>Latilumbus</i>	<i>palliventris</i>	LIT: Townes 1969	97%	extant	EU378639/HQ567619
Mesochorinae	<i>Lepidura</i>	<i>collaris</i>	LIT: Townes 1969	73%	extant	
Mesochorinae	<i>Mesochorus</i>	sp.	LIT: Townes 1969	79%	extant	MK851111/MK959434
Mesochorinae	<i>Plectochorus</i>	<i>iwatensis</i>	LIT: Townes 1969	75%	extant	EU378646/HQ548200
Mesochorinae	<i>Stictopisthus</i>	sp.	LIT: Townes 1969	75%	extant	- / KY447209
			PIN: HT 363/57, PT 964/231, NMB	73%	extant	HQ025772/MG335553
Pherhombinae	<sup>2</sup> <i>Pherhombus</i>	<i>antennalis</i>	#JDC4531	68%	amber	
Pherhombinae	<i>Pherhombus</i>	<i>brischkei</i>	NHMD 876110		fossil: Baltic	
Pherhombinae	<i>Pherhombus</i>	<i>dolini</i>	LIT: Tolkanitz et al. 2005	64%	amber	
Pherhombinae	<i>Pherhombus</i>	<i>kasparyani</i>	LIT: Manukyan 2019	42%	fossil: Rovno	
Pherhombinae	<i>Pherhombus</i>	<i>kraxtelleensis</i>	LIT: Manukyan 2019	39%	amber	
Pherhombinae	<i>Pherhombus</i>	<i>kraxtepellensis</i>	LIT: Manukyan 2019	56%	fossil: Baltic	
Pherhombinae	<i>Pherhombus</i>	sp.	NHMD 876113	59%	amber	
Pherhombinae	<i>Pherhombus</i>	<i>parvulus</i> n.sp.	FUR: #10652	18%	fossil: Fur	
Pherhombinae	<i>Pherhombus</i>	<i>sorgenauensis</i>	LIT: Manukyan 2019	46%	fossil: Baltic	
					amber	

Townesitinae	<i>Marjorietta minor</i>	NMB #JDC9020	76%	fossil: Baltic amber
Townesitinae	<i>Rasnitsynites tarsalis</i>	SMNS: BB-880-K	60%	fossil: Baltic amber
Townesitinae	<sup>2</sup> <i>Townesites mandibularis</i>	PIN: HT 364/417, PT 364/369	55%	fossil: Baltic amber

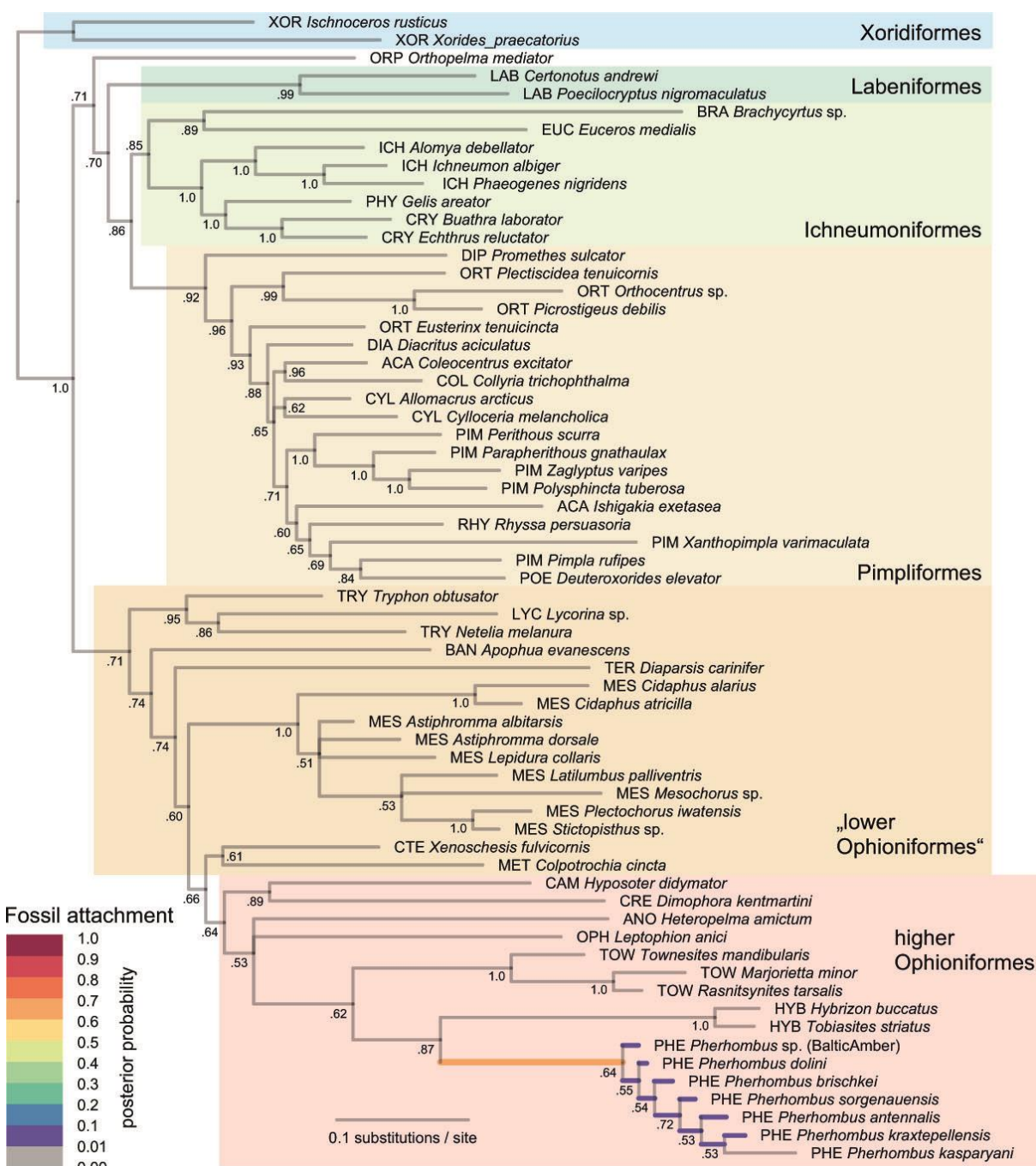
665       <sup>1</sup>Specimens or drawings used for character coding. Abbreviations: FUR = Fur Museum, Nederby, Denmark; HT = Holotype; LIT = coded from  
 666 drawing in literature; NHMD = Natural History Museum of Denmark, Copenhagen; NMB = Natural History Museum Basel, Switzerland; PIN =  
 667 Paleontological Institute, Russian Academy of Sciences, Moscow, Russia; PT = Paratype; SMNS = Staatliches Museum für Naturkunde Stuttgart,  
 668 Germany.

669       <sup>2</sup>Taxon present already in Spasojevic et al. (2021), but morphological coding expanded considerably.

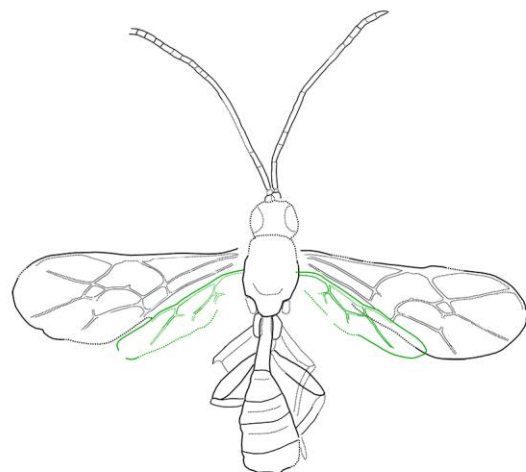
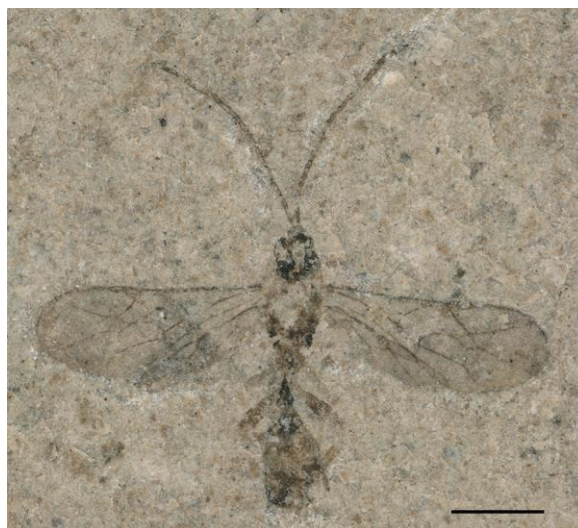


670  
671

672 Figure 1. Scatterplot of two measurements ratios, forewing veins 1-M+1-Rs / r-rs and  
673 hindwing veins 1-Rs / rs-m. The new fossil species groups together with Pherhombinae. The  
674 inlaid drawings depict the respective wing vein lengths.  
675  
676



677  
678 Figure 2. Bayesian phylogenetic analysis of combined morphological and molecular  
679 dataset, including RoguePlot showing probability of placement of *Pherhombus parvulus* n.  
680 sp. Branch colours represent posterior probabilities of attachment of the fossil to a particular  
681 branch, and support values next to nodes indicate posterior probabilities. The three-letter  
682 code in front of the taxon names denotes subfamily affiliation as follows: ACA Acaenitinae,  
683 ANO Anomaloninae, BAN Banchinae, BRA Brachycyrtinae, CAM Campopleginae, COL  
684 Collyriinae, CRE Cremastinae, CRY Cryptinae, CTE Ctenopelmatinae, CYL Cylloceriinae, DIA  
685 Diacritinae, DIP Diplazontinae, EUC Eucerotinae, HYB Hybrizontinae, ICH Ichneumoninae,  
686 LAB Labeninae, LYC Lycorininae, MES Mesochorinae, MET Metopiinae, OPH Ophioninae, ORP  
687 Orthopelmatinae, ORT Orthocentrinae, PHY Phygadeuontinae, PHE Pherhombinae, PIM  
688 Pimplinae, POE Poemeniinae, RHY Rhysinae, TER Tersilochinae, TOW Townesitinae, TRY  
689 Tryphoninae, XOR Xoridinae.  
690



691  
692

693 Figure 3. *Pherhombus parvulus* (holotype), microscope image of part 10652\_A (left);  
694 interpretative drawing based on part and counterpart (right; a photograph of the  
695 counterpart is provided as Supplementary File S4). Solid lines imply a high certainty of  
696 interpretations, while dotted lines indicate interpolations or uncertain interpretations.  
697 Hindwings are shown in green to improve clarity. Differences in line width are used to  
698 visualise small structures and do not imply varying certainty. The scale bar indicates 1 mm.